this concept are the observations in "prediabetic" man (*16*) and in the isolated perfused pancreas of normal and diabetic Chinese hamsters (*17*) which indicate almost complete restoration of glucose-induced release of insulin by theophylline derivatives in some diabetics and no enhancement in others.

M. ARTHUR CHARLES
R. FANSKA, FLORENCE G. SCHMID
PETER H. FORSHAM
GEROLD M. GRODSKY
Metabolic Research Unit, Department of Biochemistry and Biophysics, University of California Medical Center, San Francisco 94122

References and Notes

1. A. G. Robison, R. W. Butcher, E. W. Sutherland, *Cyclic AMP* (Academic Press, New York, 1971), pp. 17–46.
2. J. R. Turtle and D. M. Kipnis, *Biochem. Biophys. Res. Commun.* **28**, 797 (1967).
3. K. E. Sussman and G. D. Vaughan, *Diabetes* **16**, 449 (1967).
4. G. M. Grodsky, L. L. Bennett, D. F. Smith, F. G. Schmid, *Metabolism* **16**, 22 (1967).
5. W. J. Malaisse, F. Malaisse-Lagae, D. Mayhew, *J. Clin. Invest.* **46**, 1724 (1967).
6. L. L. Bennett and G. M. Grodsky, in *Diabetes*, J. Ostman, Ed. (Excerpta Medica Foundation, Amsterdam, 1969), p. 462.
7. W. Malaisse, F. Malaisse-Lagae, S. King, *Diabetologia* **4**, 370 (1968).
8. G. R. Brisson, F. Malaisse-Lagae, W. J. Malaisse, *J. Clin. Invest.* **51**, 232 (1972).
9. W. Montague and J. R. Cook, *Biochem. J.* **122**, 115 (1971).
10. P. E. Lacy, M. M. Walker, C. J. Fink, *Diabetes* **21**, 987 (1972). We thank Dr. Paul Lacy for his interest and encouragement, enabling us to establish a perifusion system.
11. Results with islets homogenized in 5 percent trichloroacetic acid followed by acid-ether extraction and lyophilization were comparable to islets boiled in theophylline.
12. A. G. Gilman, *Proc. Nat. Acad. Sci. U.S.A.* **67**, 305 (1970).
13. S. Porte, *J. Clin. Invest.* **48**, 2309 (1969).
14. G. M. Grodsky, L. L. Bennett, D. Smith, K. Nemechek, in *Tolbutamide after Ten Years*, W. J. H. Butterfield and W. Van Westering, Eds. (Excerpta Medica Foundation, Amsterdam, 1967), p. 11.
15. G. M. Grodsky, *J. Clin. Invest.* **51**, 2047 (1972).
16. E. Cerasi and R. Luft, *Horm. Metab. Res.* **1**, 162 (1969).
17. B. Frankel and G. M. Grodsky, in preparation.
18. We thank Drs. M. Mozen and A. Pappenhagen of Cutter Laboratories, Berkeley, Calif., and Dr. J. Holper of Abbott Laboratories, South Pasadena, Calif., for their generous assistance in providing the supplies of albumin necessary for these studies. This study was supported in part by National Institute of Allergy and Metabolic Diseases grant AM-01410 and by the Hoechst Pharmaceutical Company, Somerville, N.J.; the Levi J. & Mary Skaggs Foundation; and the Kroc Foundation. M.A.C. is a postdoctoral fellow of the U.S. Army.

20 October 1972

Automatic Screening of Biological Specimens by Optical Correlation

Abstract. *An optical analog correlation technique was used to detect morphologic abnormalities in rat liver cells. The method employs an optical matched filter for correlating a test pathological specimen with a control specimen. Experimental results show appreciable promise that such an optical correlator can be employed as a tool for rapid mass screening of a variety of pathological specimens.*

The automation of a number of laboratory procedures relevant to the study of cells and their internal structures has been successfully accomplished. There are presently available automated methods for counting erythrocytes and leukocytes, detecting circulating neoplastic cells, and differentiating normal and neoplastic cells in cytological preparations. These automated techniques are often complex and time consuming, and most require an on-line digital computer for data storage and handling. In recent years, particularly since the advent of continuous wave lasers, optical data processing techniques have found many applications in engineering (*1*) and biological fields (*2*).

The technique presented in this report performs a real time correlation between a microscopic specimen of known pathology and one of unknown pathology from the same organ of a different individual. A technique utilizing a multitude of samples (as in raster scanning) would not produce real time correlation since each sample must be stored in a memory bank and the correlation performed only after sufficient data points to represent the entire specimen have been stored. A raster of sufficient resolution to analyze this specimen would divide the specimen into approximately 2000 scan lines each consisting of 2000 points with intensities relating to the intensities of the points in the original specimen. A large area or an entire section of the organ can be instantaneously inspected at one time, which eliminates the need for raster scanning of the specimen. The maximum area of inspection can be as large as a standard microscope slide. The possibility of automatic screening of biological specimens by an optical character recognition process stems from the fact that cells and tissue often react to disease or injury by undergoing morphological changes which are similar for a particular pathogen or injury in a particular organ. Examples of morphological changes are cellular swelling, cytoplasmic and nuclear degeneration, and cytokinesis (cytoplasmic changes during cell division). This cytomorphosis produces significant changes in the light scattering characteristics of the specimen. The optical matched filtering technique permits high signal-to-noise ratio detection of such morphological changes. The process in its present state of development is essentially a generalized formulation of the Weiner optimum filtering theory (*3*), which is easily realized in optical data processing.

The methodologies of coherent optical correlation are well documented (*4*). The experimental arrangement used in the study reported here is shown schematically in Fig. 1. A microscope slide containing a normal rat liver specimen, prepared by a standard hematoxylin and eosin staining process, is placed in the input plane (x, y). The function $f(x, y)$ denotes the amplitude transmission function of the object when it is illuminated by a collimated beam of coherent light. The lens L_1 focuses the two-dimensional

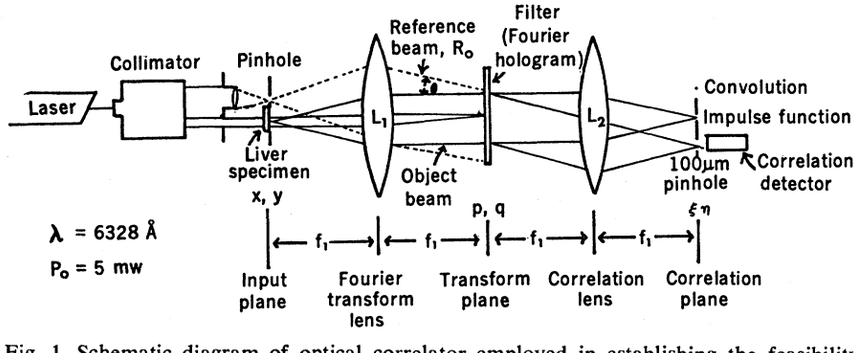

Fig. 1. Schematic diagram of optical correlator employed in establishing the feasibility of automatic detection of morphologically abnormal rat livers. The reference beam, represented by the dashed lines, is blocked off during the correlation measurements.

Fourier transformation resulting from the Fraunhofer diffraction of light by the specimen $f(x, y)$ onto the back focal plane (p, q). This transformation $F(p, q)$ is represented mathematically by

$$F(p,q) = \iint f(x,y) \exp\left[\frac{2\pi i(px + qy)}{\lambda f_1}\right] dxdy$$

where λ is the wavelength of the coherent light and f_1 is the focal length of lens L_1. A reference beam R_0 is superimposed on this Fourier transform in the (p, q) plane at an angle θ, and the resultant light intensity modulation, represented mathematically by $H(p, q)$, is recorded on a Kodak 649-F spectroscopic plate. The Fourier hologram $H(p, q)$ generated in this process contains amplitude and phase information of the spatial frequency spectrum $F(p, q)$ of the control specimen (*4*). The Fourier hologram filter is photographically processed, and is then positioned in its original location. During the correlation studies, the test specimen $s(x, y)$ is placed in the input plane and the reference beam R_0 is blocked off. The Fourier transform $S(p, q)$ of the test object is multiplied by the photographically recorded Fourier transform $F(p, q)$ of the transmission function $f(x, y)$. The lens L_2 (also of focal length f_1) takes the inverse transform of this product to produce the optical analog of the desired correlation function

$$\iint F^*(p,q)\, S(p,q) \exp\left[\frac{2\pi i(p\xi + q\eta)}{\lambda f_1}\right] dpdq = \iint f^*(x,y)\, x(x + \xi, y + \eta) dxdy = R_{fs}$$

where the asterisk signifies the complex conjugate, R_{fs} is the cross-correlation function, and ξ and η are coordinates in the correlation plane. When the optical transmission functions of the input objects are normalized, the center of the correlation function in the correlation plane (ξ,η) has its highest light intensity value (autocorrelation) only when $f(x, y) = s(x, y)$. A significant decrease in the correlation function indicates a difference between the spatial structure of the test specimen and that of the control specimen that was used to record the holographic matched filter.

A 5-mw He-Ne laser was used as the coherent light source. A 100-μm aperture was centered about the correlation term (Fig. 1), and a photomultiplier was used to detect the maximum intensity of light passing through the aperture. This light intensity maximum corresponds to the high correlation components of the correlation function. The filtering process is insensitive to minor variations in the location and orientation of the test sections in the input plane, but is extremely sensitive to the position of the Fourier hologram matched filter in the (p, q) plane.

It is often necessary to increase discrimination between signal inputs from specimens having similar morphologies. One way to enhance the difference between specimens is to remove spatial frequencies that are common to all the specimens tested. For example, the aperture in the input plane will have its own spatial frequency spectrum superimposed on the spatial frequency spectra from both control and test objects. Increased discrimination was implemented by first exposing the photographic plate to the frequency spectrum of the aperture, thus masking out these terms during correlation. The high spatial frequencies were emphasized by slightly overexposing the photographic plate to $F(p, q)$, resulting in an attenuation of the higher light intensities during the subsequent correlation process. These high light intensities correspond to low spatial frequency components.

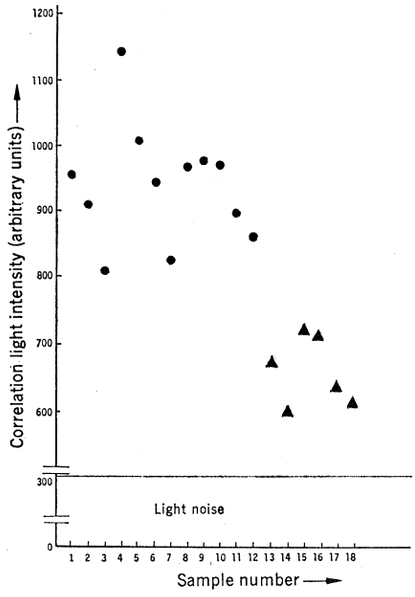

Fig. 2. Scatter diagram demonstrating the correlation obtained between various rat liver specimens and a normal liver specimen by utilizing the correlator shown in Fig. 1. (Circles) Normal control rat liver; (triangles) livers of injected rats, exposed for 48 hours. Each correlation reading is the average for four positions on each liver specimen.

Adult Sprague-Dawley rats received an intraperitoneal injection of carbon tetrachloride. The animals were killed 48 hours later and slides prepared by hematoxylin-eosin staining were made for the livers of injected and control rats. The halogenated hydrocarbon caused prominent vacuolation of hepatocytes, especially in the centrilobular areas. In the correlation studies, all the control specimens showed a high degree of correlation, whereas the abnormal specimens showed a significantly lower degree of correlation. A typical scatter diagram showing the relative correlation between a normal specimen and all other normal and abnormal specimens in a particular population is shown in Fig. 2.

These findings lead to the following tentative conclusions. Optical matched filtering can be advantageously employed for mass screening of certain biological specimens. A large area or the entire specimen can be examined at one time for instantaneous identification and decision, whereas examination with a microscope requires a detailed scanning process over numerous small areas. The correlator can be adapted so that there are no false positive readings, while some false negative readings may occur but can be tolerated. The data presented in Fig. 2 represent a population of liver specimens in which false negative readings did not occur, although it is possible that false negative readings may occur in some other specimen populations. The correlator has a fast screening rate. In a research program where rapid and reliable screening of a large number of pathological samples is needed, this automatic optical screening technique could reduce considerably the time spent by laboratory technicians.

R. L. Bond, M. K. Mazumder
M. K. Testerman, D. Hsieh
Department of Electronics and Instrumentation, Graduate Institute of Technology, University of Arkansas, Little Rock 72203

References and Notes

1. R. A. Binns, A. Dickinson, B. M. Watrasiewicz, *Appl. Opt.* **7**, 1047 (1968); E. Marom, *Laser Focus* **5** (No. 19), 43 (1969).
2. E. Feleppa, *Phys. Today* **22** (No. 7), 25 (1969); A. Brunsting and P. F. Mullaney, *Appl. Opt.* **11**, 675 (1972); A. L. Hammond, *Science* **174**, 1011 (1971).
3. Y. W. Lee, *Statistical Theory of Communication* (Wiley, New York, 1960), p. 440.
4. For example, see J. W. Goodman, *Introduction to Fourier Optics* (McGraw-Hill, New York, 1968), p. 141; A. Vander Lugt, *IEEE (Inst. Elect. Electron. Eng.) Trans. Inf. Theory* **IT-10**, 139 (1964).
5. The work on which this report is based was

performed pursuant to contract FDA 71-97 with the National Center for Toxicological Research. The authors wish to thank Dr. William E. Jaques, chairman of the Department of Pathology, University of Arkansas Medical Center, for his review of this report and his constructive and critical comments on the pathological aspects of the research.

23 June 1972; revised 17 November 1972

Fine Structure of Muscle Cells of the Human Testicular Capsule: Basis of Testicular Contractions

Abstract. *Electron micrographs of human testicular capsule reveal large numbers of branching smooth muscle cells coursing through collagenous tissue of the tunica albuginea. These cells have subcellular morphology characteristic of smooth muscle cells, and they associate with one another through areas of close contact. These are the contractile cells responsible for spontaneous contractions of the human testicular capsule—contractions that may be important in transporting nonmotile sperm out of the testis.*

Confining the seminiferous tubules and interstitial tissue of the human testis is a capsule commonly referred to as the tunica albuginea. It has been described as a dense connective tissue consisting mainly of fibroblasts and collagen; like the capsules of other organs, the testicular capsule is considered to act as a support for the underlying parenchymal tissue.

Recently Davis and Langford (*1*) reported that the human testicular capsule is capable of spontaneous contractions and that it can be stimulated to contract by several autonomic drugs. These observations suggest that the capsule may indeed be more than an outer support for the testis. In animals, they were able to demonstrate not only contractions of the capsule but also similar contractions of the intact whole testis both in vitro and in the living animal (*1*, *2*). The possibility that smooth muscle cells may be responsible for these contractions became evident when cells resembling smooth muscle cells were found with the light microscope in the capsules of animal and human testes (*1–3*). Electron microscopy studies were therefore undertaken to define the cells responsible for the contractions of the capsule. We report here the fine-structural identification and morphology of the contractile cells located in the capsule of the human testis.

Biopsy specimens of the testicular capsule from young, healthy, adult volunteers were obtained. Capsule tissue was immediately transferred to glutaraldehyde, postfixed in osmium tetroxide, dehydrated in ethanol, and embedded in Epon (*4*). To improve contrast of membranes, some specimens were stained en bloc prior to embedding in Epon (*5*). Thin sections were doubly stained with uranyl acetate and lead citrate (*6*).

The three tissue layers of the human testicular capsule can readily be identified by light microscopy (*1*, *2*). The exterior tunica vaginalis visceral consists of a thin layer of serous cells. Directly beneath is the tunica albuginea, a dense collagenous tissue forming the major portion of the capsule. The interior tunica vasculosa is less dense than the

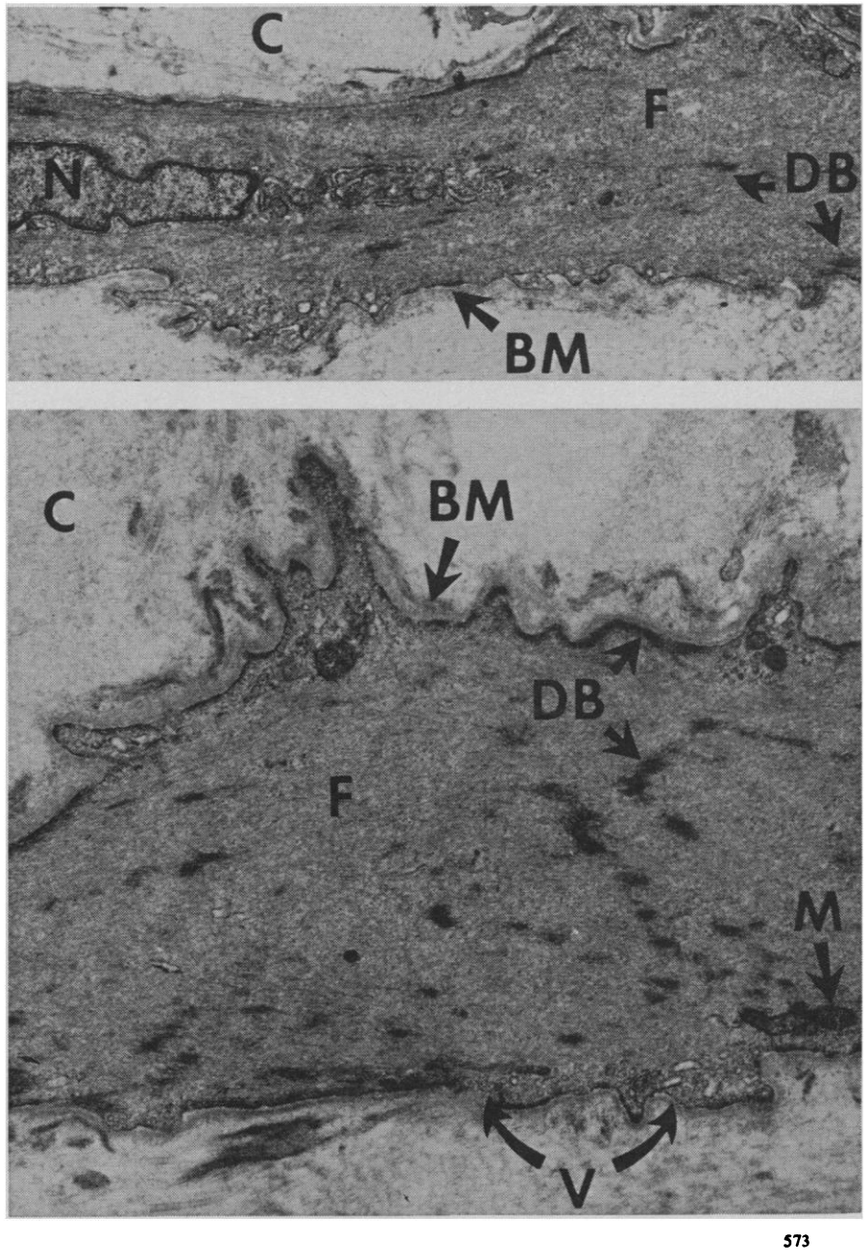

Fig. 1. Electron micrographs of smooth muscle cells (longitudinal section) located in the tunica albuginea of the human testicular capsule. (Top) A smooth muscle cell is surrounded by collagen (*C*). Myofilaments (*F*), dense bodies (*DB*), and a basement membrane (*BM*) can be seen. Most of the organelles extend from the poles of the nucleus (*N*) (× 9,900). (Bottom) Cytoplasm of the smooth muscle cells contains mainly myofilaments (*F*) and dense bodies (*DB*). Numerous micropinocytotic vesicles (*V*) are located at the cell periphery along with occasional mitochondria (*M*) (× 10,300).